LARGE EDDY SIMULATION OF THE INFLUENCE OF HIGH FREE-STREAM TURBULENCE ON SPATIALLY EVOLVING BOUNDARY LAYER

Frédéric Péneau and Henri Claude Boisson
Institut de Mécanique des Fluides de Toulouse, av Pr Camille Soula,
31400 Toulouse FRANCE

Ned Djilali
Department of Mechanical Engineering, University of Victoria,
Victoria, B.C. V8W 3P6 CANADA

ABSTRACT

The influence of a high free-stream turbulent field on a spatially evolving turbulent flat plate boundary layer is investigated using a Large Eddy Simulation (LES) with a dynamic mixed subgrid-scale model. The evolution of skin friction, heat transfer coefficient, flow and thermal field are presented. The impact of free-stream turbulence on shear stress and velocity profiles is minimal; whereas substantial heat transfer augmentations are predicted together with a modification of the temperature profiles in the logarithmic and wake regions.

1 INTRODUCTION

Our understanding of the turbulent mechanisms and interactions between the large scale structures in a turbulent boundary layer and the small dissipative structures is limited. The influence of a very high free-stream turbulence on these interactions is even less well understood, despite the numerous experimental studies undertaken these last twenty years [Maciejewski & Moffat(1992)], [Blair(1983)], and [Hancock & Bradshaw(1989)].

This type of flow is indeed one of the most important industrial heat transfer problems. Recent studies have shown that the thermal field is more sensitive to the free-stream turbulence than the dynamic field [Maciejewski & Moffat(1992)]. This difference in behavior underscores that the relationship between the temperature and velocity field is more complex than implied by the passive scalar approach.

The improved version of [Zang *et al.*(1993)] of the "dynamic subgrid-scale eddy viscosity model" [Germano *et al.*(1991)] was used in the present simulations. This dynamic mixed model (DMM) computes locally the subgrid viscosity and diffusivity allowing the model to not only capture the energy backscatter of the small eddies towards the large ones, but also to exhibit the correct asymptotic behavior in the vicinity of solid walls without having to resort to a damping function. This latter feature of the model allows us to undertake the study of the influence of a high free-stream turbulent on the dynamic and heat transfer coefficients, since these are not imposed via an assumed law.

Many of the Direct and Large Eddy Simulations (LES) of turbulent flows performed to date are temporal simulations (channel flow, mixing layer). For the problem of interest here, one can not perform a temporal simulation, since there is no periodicity in the streamwise direction. Consequently, we undertook a spatial simulation of a flat plate turbulent boundary layer, and had therefore to deal with the problem of open exit and entrance boundary conditions. Whereas open boundary conditions are well documented in the literature, very little information is available for on the prescription of entrance conditions. The problem is that, strictly, it is necessary to prescribe a velocity field with the correct turbulent energy spectrum as well as the correct spatial coherence. An inlet condition based on Linear Stochastic Estimation (LSE) of velocity time histories has been implemented for this study. This approach allows us to obtain a fully turbulent flat plate boundary layer from the beginning of the domain. The longitudinal domain length that is required is thereby substantially reduced and the major part of the calculation box is devoted to the analysis of the problem rather than to the development of the flow. This new entrance condition will not be presented in this paper, but readers are referred to [Péneau *et al.*(1999*a*)] for a detailed presentation and to [Péneau *et al.*(1999*b*)] for

a discussion of the turbulent boundary layer simulations obtained with this inlet condition for the case of zero free-stream turbulence.

After a brief description of the numerical method and the Dynamic Mixed Model (DMM) in Sec. 2, we will present the method adopted to obtain the free-stream turbulent fields and discuss the physical features and characteristics of these fields. Finally, in Sec. 4, we present the first results obtained on the influence of high free-stream turbulence on the thermal and velocity field.

2 NUMERICAL METHOD AND SUBGRID MODELLING

2.1 The numerical method

The numerical simulations are carried out using the JADIM code. The two dimensional version of this code has been fully described by [Magnaudet *et al.*(1995)] and the three dimensional one by [Calmet & Magnaudet(1996)]; we only present here a summary of the numerical method. The momentum and scalar equations are discretized using finite volume method with a second-order centered schemes on a staggered grid. The solution is advanced in time using a three-step Runge-Kutta (RK) procedure. The nonlinear terms of each equations are computed explicitly while the diffusive terms are calculated using the semi-implicit Crank-Nicholson (CN) algorithm. This latter feature is particularly important for resolving the near-wall region without prohibitively small time steps to maintain numerical stability. To satisfy the incompressibility conditions, a Poisson equation is solved by combining a direct inversion in the (x_1, x_2) plane with a spectral Fourier method in the x_3 direction. The old version of JADIM uses a multigrid method for the third direction. This method which works well in many flows, seems to fail on the case of the spatially evolving turbulent flow. The use of a spectral Fourier method, implying periodicity in the spanwise direction, not only increased accuracy but also results in significantly faster computations.

2.2 The LES equations and the subgrid-scale model

The governing equations for Large Eddy Simulation result from a spatial filtering of the Navier-Stokes equations. Since we used a finite volume method, the filter is imposed by the discretization and corresponds to the box-filter $\bar{G}\left(x_i^{'} - x_i\right) = 1$ if $\left|x_i^{'} - x_i\right| \leq \bar{\Delta}_i$ and 0 otherwise, where $\bar{\Delta}_i$ is the local mesh spacing in the x_i direction. This explicit filtering is one of the attractive features of this model since no averaging of the resolved field is required. Decomposing the velocity field into a resolved part $\overline{V}_i$ (directly computed by the code) and a subgrid part $V_i^{'}$ (the unknown in the equations), i.e. $V_i(\vec{x},t) = \overline{V}_i(\vec{x},t) + V_i^{'}(\vec{x},t)$. We obtain the following system of equations :

$$\begin{cases} \frac{\partial \overline{V}_i}{\partial x_i} = 0 \\ \frac{\partial \overline{V}_i}{\partial t} + \frac{\partial \overline{V}_i \overline{V}_j}{\partial x_j} = -\frac{\partial \overline{p}}{\partial x_i} + \frac{\partial \left[2(\nu+\nu_t)\overline{S}_{ij} - L_{ij}\right]}{\partial x_j} \\ \frac{\partial \overline{T}}{\partial t} + \frac{\partial \overline{T}\,\overline{V}_j}{\partial x_j} = \frac{\partial \left[(D+D_T)\partial \overline{T}/\partial x_j - Lc_j\right]}{\partial x_j} \end{cases} \quad (1)$$

where:

$$\text{a) } L_{ij} = \overline{\overline{V}_i \overline{V}_j} - \overline{\overline{V}_i}\,\overline{\overline{V}_j} \qquad \text{b) } Lc_j = \overline{\overline{T}\,\overline{V}_j} - \overline{\overline{T}}\,\overline{\overline{V}_j} \quad (2)$$

$$C_{ij} = \overline{\overline{V}_i V_j^{'}} + \overline{\overline{V}_j V_i^{'}} - \left(\overline{\overline{V}_i}\,\overline{V_j^{'}} + \overline{\overline{V}_j}\,\overline{V_i^{'}}\right) \quad (3)$$

$$Cc_j = \overline{\overline{T} V_j^{'}} + \overline{\overline{V}_j T^{'}} - \left(\overline{\overline{T}}\,\overline{V_j^{'}} + \overline{\overline{V}_j}\,\overline{T^{'}}\right) \quad (4)$$

$$\text{a) } R_{ij} = \overline{V_i^{'} V_j^{'}} - \overline{V_i^{'}}\,\overline{V_j^{'}} \qquad \text{b) } Rc_j = \overline{T^{'} V_j^{'}} - \overline{T^{'}}\,\overline{V_j^{'}} \quad (5)$$

$$\overline{p} = \overline{P} + (C_{kk} + R_{kk})/3 \quad (6)$$

L_{ij}, Lc_j are calculated explicitly. The cross terms C_{ij}, Cc_j and R_{ij}, Rc_j on the other hand cannot be computed directly since $V_i^{'}(\vec{x},t)$ is unknown. Accordingly, these terms are modeled using the classical concepts of subgrid viscosity and diffusivity [Smagorinsky(1963)] in conjunction with the DMM of [Zang *et al.*(1993)]. C_{kk} and R_{kk} are incorporated into the pressure terms because the incompressibility condition renders the evaluation of $(C_{kk} + R_{kk})$ impossible. The subgrid viscosity $\nu_t = f(\vec{x},t)$ and diffusivity $D_T = f(\vec{x},t)$ are calculated every time step at each computational volume of the domain. For further details on the DMM and the calculation procedure for evaluating the subgrid viscosity and diffusivity, the reader is referred to the paper of [Péneau *et al.*(1999*b*)].

2.3 Grid and physical parameters

Taking into account the problem of open boundary conditions, the dimensions of the domain are: $L_x = 85\delta_1, L_y = 50\delta_1, L_z = 20\delta_1$, where δ_1 is the displacement thickness at the entrance of the domain. The number of points in each direction are: $N_x = 96, N_y = 96$ and $N_z = 64$. In wall units, the mesh size in the longitudinal and spanwise directions are: $\left(\Delta x^+, \Delta z^+\right) = (38, 24)$. On the direction normal to the wall, the mesh is refined. The first point is at $y^+ = 0.18$. The Reynolds number at the entrance, based on δ_1 is $\mathrm{Re}_{\delta_1} = 1620$. The boundary layer thickness at the entrance of the domain is $\delta = 0,16m$. We simulate an air flow, therefore $\mathrm{Pr} \simeq 0.72$. The mean free-stream velocity is $U = 1.23m/s$, while the temperature of the free-stream flow is set at $T = 293°K$. The wall temperature is $T = 294°K$. All these characteristics are for the turbulent boundary layer without free-stream turbulence.

3 THE HIGH FREE-STREAM TURBULENCE FIELD

3.1 Generation

To generate a high free-stream velocity field, we start from an initial field composed of Oseen vortices of random radii R and circulation Γ. For a spanwise vortex, the velocity field is expressed by :

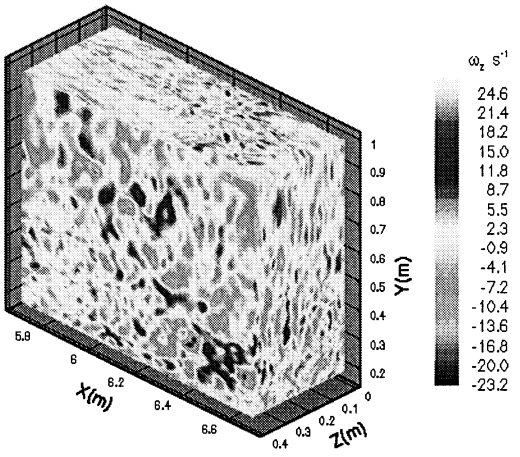

Figure 1: Typical High free-stream turbulent field

$$u = \Gamma \exp\left[\frac{-\left([x-x_0]^2+[y-y_0]^2\right)}{2R^2}\right]\frac{[y-y_0]}{R^2} \quad (7)$$

$$v = -\int \frac{\partial u}{\partial x} dy \quad (8)$$

where x and y are the coordinates along and normal to the plate. The radius R is chosen not to exceed $\left(\frac{\delta}{2}\right)$ [1], where δ is the thickness of the turbulent boundary layer[2] under the free-stream turbulence field. The lower bound for R is set at twice the local mesh size, which ensures that at least four cells define the vortex in a given plane. The circulation is chosen in the range $\frac{\Gamma}{R} \in [-b; b]$ where the value of b depends on the desired turbulent intensity. Only longitudinal ω_x and spanwise ω_z vortices are generated.

Once the initial velocity field has been obtained, we start the calculation with periodic condition in the longitudinal and spanwise direction and constant velocity at the upper and lower limit of our domain. The latter boundary condition corresponds to the flat plate turbulent boundary layer condition at $(y = \delta)$ where $u = 1.23m/s$ [3], $v = w = 0m/s$. A typical velocity field obtained after a sufficient number of time steps is illustrated in figure 1. To introduce this field into the computational domain of the flat plate turbulent boundary layer, we record (y, z) plane time histories of this free-stream turbulence field; these are then used in conjunction with the Linear Stochastic Estimation (LSE) [Péneau *et al.*(1999*b*)] to construct time-dependent entrance conditions for the simulation of the flat plate turbulent boundary layer.

[1] This does not imply that at the end the free-stream turbulent field has no structure bigger than δ, because of possible pairing and merging.

[2] For our problem, $\delta \simeq 0.17m$

[3] This study is undertaken in collaboration with INRA for heat transfer in refregiration chamber. Typical velocity is around $1m/s$.

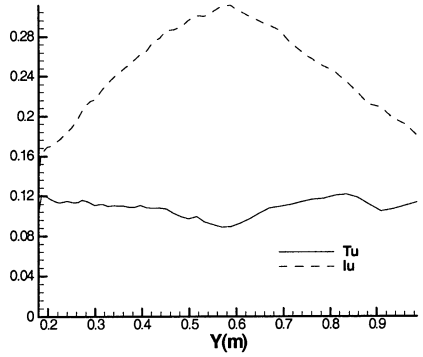

Figure 2: Typical turbulent intensities profiles

3.2 Characteristics

On figure 2, we present typical turbulent intensities profiles where $Tu = u_{rms}/U$ and $Iu = \sqrt{u'^2+v'^2+w'^2}/\left\|\overrightarrow{U}\right\|$, where U is the local mean velocity value. The evolution of Iu is consistent with the boundary condition imposed on the free-stream turbulence, i.e. constant velocity along the top and bottom of the domain. This implies that the fluctuations of the normal velocity v vanish when approaching these boundaries. As we move away from the constant velocity boundaries, the v_{rms} increases, reaching a maximum in the middle of the domain, hence the shape of the Iu profile. The mean U velocity profile for the free-stream turbulence field was fixed to a constant mean value of $1.23m/s$ within a accuracy of $\pm 3\%$ on a distance of δ above the boundary layer. This was motivated by the high sensitivity of the turbulent boundary layer to the mean pressure gradient imposed by the free-stream turbulent field observed in earlier simulations. Indeed, the first simulations undertaken with a free-stream turbulent field with a mean velocity at the interface10% below the external velocity U_e at $Tu = 0\%$ showed a clear reduction of the skin friction coefficient. Examination of the longitudinal and transverse spectra shows that the turbulence field is neither homogeneous nor isotropic. This conclusion is confirmed by the turbulent intensities profiles. To the question of how realistic is such turbulent field, we observe that the time evolution of the field's statistics shows a decrease of the turbulent intensities as in grid turbulence. An expression of the form $K(t-t_0)^{-n}$ with $n \simeq 1$ provides a good fit for these time evolutions.

The major difference between the experimental conditions and the present simulations, is that the turbulent flat plate boundary layer has not developed under the free-stream turbulent field. This results in the u_{rms} profile evolution shown on figure 3. For our simulations, the turbulent flat plate boundary layer "senses" the presence of the turbulent field progressively. Three sim-

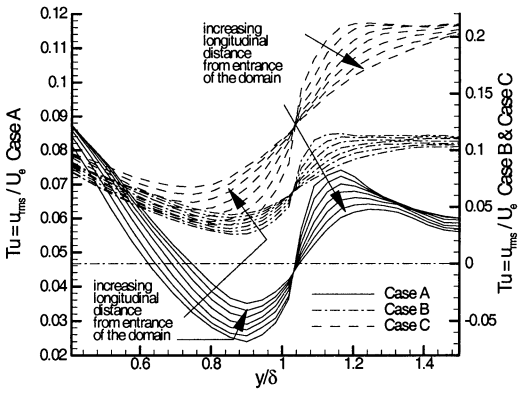

Figure 3: Typical longitudinal u_{rms} profiles evolution

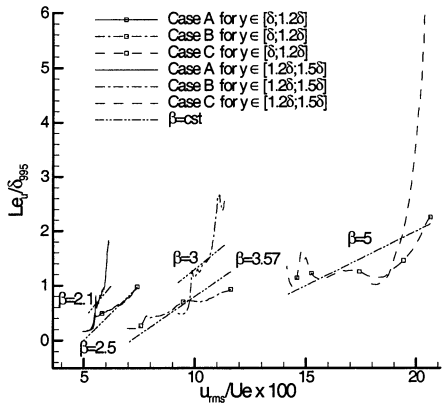

Figure 4: Sample free-stream turbulent field dissipation length-scale and turbulent intensities

ulations are presented on figure 3. They correspond to different levels of external turbulent intensities. There is obvious difficulty in determining which value is significant in driving the transfer of the turbulent boundary layer. A strong decrease of u_{rms} is observed just above the boundary layer while at about $[0.8\delta;\delta]$ the opposite happens. It appears that there is not a unique manner of characterizing the interaction mechanism. Moreover, it might be expected that the dissipation length-scale seen by the boundary layer increased with streamwise distance. The evolution of the dissipation length-scale of the free-stream turbulent field, $Le_u = \frac{-\overline{u'^2}^{3/2}}{U d\overline{u'^2}/dx}$, is presented in figure 4 for some of the cases treated where $\beta = Tu/\left(Le_u/\delta_{995} + 2\right)$. On this figure, we can see that a large range of length-scale is represented. Nevertheless, the representativeness of these dissipation length scales is questionable as it depends on the interval on which the length is integrated. Two sets of characteristic length are indeed presented. One corresponds to the external field and the other to the interaction region. For the same condition, they correspond to quite different value. Moreover, the intermittency of the boundary layer free-stream turbulence interface can be involved so that it is difficult to say which length-scale is seen by the boundary layer.

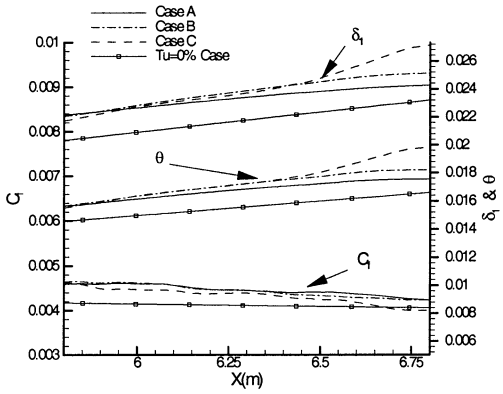

Figure 5: Influence of the free-stream turbulence on the dynamic characteristic of the TBL

4 RESULTS

The interpretation of the results is quite difficult if we restrict our analysis to what has been done in experiments. Indeed, as we point it out in section 3.2, the turbulent field penetrates progressively the boundary layer. If we look at figure 5, we can see that the influence of the free-stream turbulence is important at the entrance of the domain and then progressively diminishes. The increase of C_f at the entrance of the domain may be explained by the adaptation of the flow to its new outside boundary layer condition.

The fact that for all the free-stream turbulence intensity investigated here the increase in friction coefficient is about the same, is surprising. This is grist to mill of those who believe that free-stream turbulence does not influence the dynamic properties of the boundary layer. Figure 6 shows that, except for a slight decrease in the logarithmic slope is observed, we may conclude that the mean velocity profile is not perturbed by the free-stream turbulence. This is not the case for the temperature field. Figure 7 shows that the evolution of the Stanton number follow the one of the friction coefficient for $X \leq 6.2m$. Consider the expression of the Stanton number: $St = \frac{q''_w}{\rho U_\infty c_p (T_w - T_\infty)} = \frac{T^* u_t}{U_\infty (T_w - T_\infty)}$ where T^* is obtained from $T^+ = \Pr y^+$ and $T^+ = \frac{T_w - T}{T^*}$. The predicted drop is consistent with the above expression if we assume that the thermal interaction between the free-stream turbulence and the boundary layer is weak at the entrance. This weak interaction is not in con-

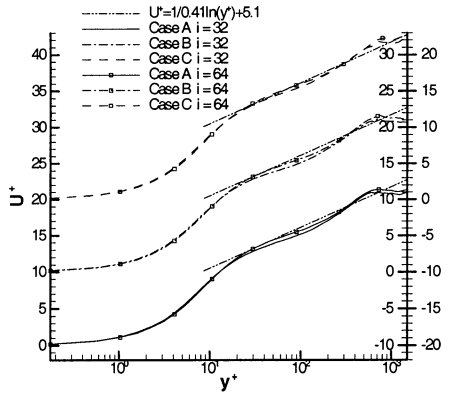

Figure 6: Influence of the free-stream turbulence on the mean velocity profile

tradiction with what has been said on the necessary dynamic adaptation of the flow at the entrance, as for the temperature, the turbulent free-stream is assume to be at constant temperature.

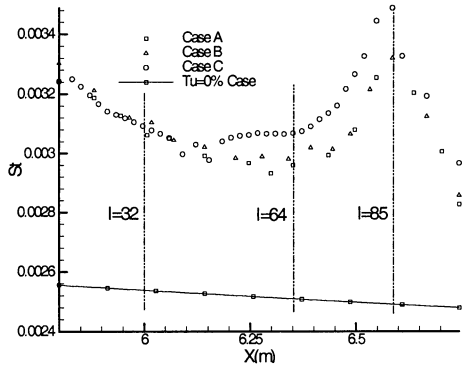

Figure 7: Influence of the free-stream turbulence on heat transfer coefficient

The more interesting feature in figure 7 is the rapid increase of the Stanton number for $6.2m \leq X \leq 6.65m$. A net influence of the free-stream turbulent intensity is then observed and may be associated to a strong thermal interaction between the free-stream and the boundary layer.

Examining at the temperature profiles in figure 8, we note that the behavior of the thermal field reported experimentally by [Maciejewski & Moffat(1992)] is reproduced in our simulations. The different thickness presented on figure 9 are polynomial fitted curved with a maximum deviation being 3%. When compared to the dynamic thickness presented in figure 5, the notion of weak and strong interaction becomes obvious. Indeed

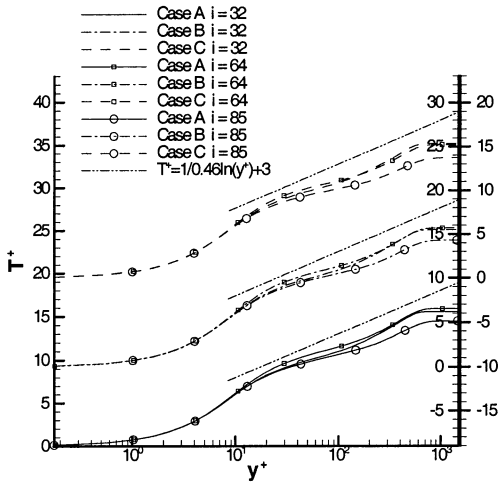

Figure 8: Influence of the free-stream turbulence on the mean temperature profile

a significant increase is observed for various characteristic thicknesses for enthalpy $\Delta = \int_0^{\delta_T} \frac{U}{U\infty}\left(\frac{T_w - T}{T_w - T_\infty}\right) dy$; energy $\delta_3 = \int_0^{\delta_T} \frac{U}{U\infty}\left(1 - \left(\frac{U}{U\infty}\right)^2\right) dy$; and the thermal boundary thickness δ_T defined as the distance where $T = 0.005T_w$.

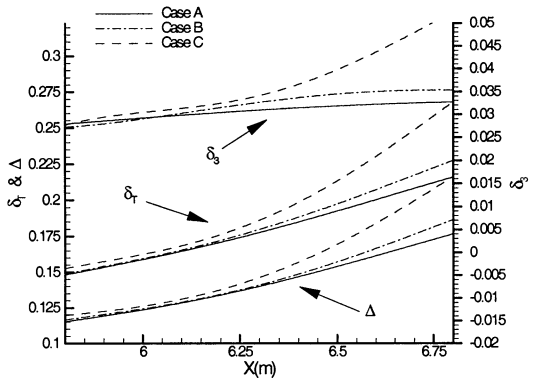

Figure 9: Influence of the free-stream turbulence on the thermal characteristic of the TBL

The rapid fall of the Stanton number for $X \geqslant 6.65m$ is a numerical artifact due to the increase of the longitudinal mesh size, resulting in numerical dissipation of the thermal and dynamic fluctuations.

In figure 10, we present the turbulent energy production profiles for the three different free-stream turbulent intensities. These profiles are compared to the result obtained with the same code for the case of $Tu_\infty = 0\%$.

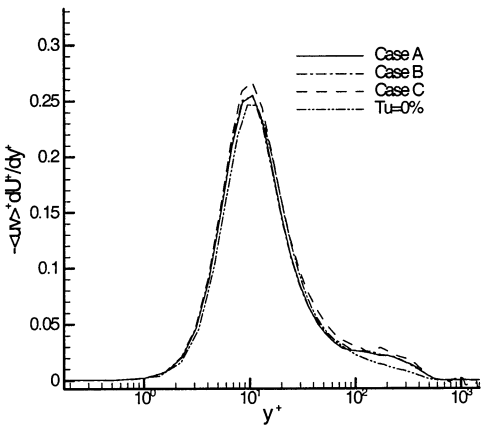

Figure 10: Influence of the free-stream turbulence on the turbulent energy production profile at i=64

The increase in the peak of production is not significant, and we note that despite the slight increase in the friction coefficient ($\approx$ 10%), the peak of production is still at $y^+ = 12$. The most important feature, is the noticeable relative increase of the turbulent energy production in the logarithmic region and in the wake. The correlation with the $\langle uv \rangle$ profiles (not shown here for lack of space), indicates that the increase in turbulent energy production is due to a reorganization of the free-stream structures penetrating the boundary layer. Indeed, in the logarithmic and wake regions $\langle uv \rangle \gg \langle uv \rangle_\infty$, where $\langle uv \rangle_\infty$ is the mean value of the correlation $\langle uv \rangle$ in the free-stream turbulent field.

5 CONCLUSIONS

Large-eddy simulations of a spatially evolving boundary layer under high free stream turbulence were under taken using a dynamic mixed subgrid scale model allowing integration to the wall. An effective method for generating free stream turbulence and inlet boundary conditions are presented. Several factors make the analysis and interpretation of the results difficult. The problem in estimating the dissipation length scale perceived by the boundary layer was discussed. In agreement with experimentally observed trends, the simulations indicate a much greater sensitivity of the thermal field to the free stream. The progressive penetration of the free stream turbulence into the boundary layer may explain the relative insensitivity of the dynamic boundary layer to free-stream turbulent intensity. To further investigate this issue, new simulations are underway where part of the free-stream turbulent field is forced to penetrate the boundary layer. Whereas the velocity profiles remain essentially unperturbed, the temperature profiles exhibit a disappearance of the logarithmic region as well as a noticeable increase in the wake region with increasing free-stream turbulent intensity. This is accompanied, in the second half of the flow, by a rapid increase in the wall heat transfer coefficient as well as the characteristic thicknesses of the thermal boundary layer. Based on preliminary analysis of the various correlations, it appears that the augmentation of the Stanton number correlates with $\langle tv \rangle$. New simulations are underway with modified boundary layer entrance conditions that should allow upstream extension of the strong interaction region observed for the thermal field, and a clarification of the impact of free-stream turbulence on the flow field.

ACKNOWLEGMENT

This work was part of a joint program INRA-CNRS and a BDI grant awarded to F. Péneau is gratefully acknowledged. We thank D^r A. Kondjoyan for his fruitful contributions. We also thank our colleagues D^r J. Magnaudet and D^r D. Legendre for their contribution to the numerical part.

REFERENCES

Blair, M. F., 1983, "Influence of free-stream turbulence on turbulent boundary layer heat transfer and mean profile development, part II- analysis of results," *Journal of Heat Transfer* **105**, pp. 41-47.

Calmet, I. & Magnaudet, J., 1996, "Large eddy simulation of high-schmidt number mass transfer in a turbulent channel flow," *Physics of Fluids* **9** (2), pp. 438-455.

Germano, M., Piomelli, U., Moin, P. & Cabot, W. H., 1991, "A dynamic subgrid-scale eddy viscosity model," *Physics of Fluids* **A3** (7), pp. 1760-1765.

Hancock, P. E. & Bradshaw, P., 1989, "Turbulence structure of a boundary layer beneath a turbulent free stream," *J. Fluid Mech.* **205**, pp. 45-76.

Maciejewski, P. K., & Moffat, R. J., 1992, "Heat transfer with very high free-stream turbulence : Part II analysis of results," *ASME Journal of heat transfer* **114**, pp. 834-839.

Magnaudet, J., Rivero, M. & Fabre, J., 1995, "Accelerated flows past a rigid sphere or a spherical bubble. Part I steady straining flow," *J. Fluid Mech.* **284**, pp. 97-135.

Péneau, F., Faghani, D. & Boisson, H. C., 1999a, "Influence of the entrance condition on the spatial development of a turbulent boundary layer," *Pre-publication EMT2, IMFT (to be published).*

Péneau, F., Legendre, D., Magnaudet, J. & Boisson, H. C., 1999b, "Large eddy simulation of a spatially growing boundary layer using a dynamic mixed subgrid-scale model," *Symposium ERCOFTAC on Direct and Large Eddy Simulation, Cambridge May 1999.*

Smagorinsky, J., 1963, "General circulation experiments with the primitive equations," *Mon. Weather Rev.* **93**, pp. 99.

Zang, Y., Street, R. L. & Koseff, J. R., 1993, "A dynamic mixed subgrid-scale model and its application to turbulent recirculating flows," *Physics of Fluids* **A5** (12), pp. 3186-3196.